Labeling of Live Cells

DOI: 10.1002/anie.200906120

Bioorthogonal Turn-On Probes for Imaging Small Molecules inside Living Cells**

*Neal K. Devaraj, Scott Hilderbrand, Rabi Upadhyay, Ralph Mazitschek, and Ralph Weissleder**

Bioorthogonal "click" reactions are now widely used in chemical biology for many applications such as activity-based protein profiling, monitoring cell proliferation, generating novel enzyme inhibitors, monitoring the synthesis of newly formed proteins, identifying protein targets, and studying glycan processing.[1,2] Arguably, the most fascinating applications involve using these bioorthogonal chemistries to assemble molecules in the presence of living systems such as live cells or even whole organisms.[3,4] These latter applications require that the chemistry does not employ toxic metal catalysts and maintains kinetics that enable fast reaction to occur with micromolar concentrations of reagents in a time span of minutes to hours. To fulfill these criteria, various "copper-free" click reactions have been reported, such as the strain-promoted azide–alkyne cycloaddition and the Staudinger ligation, to react with azides on the surface of live cells both in culture and with in vivo systems such as mice and zebrafish.[4] However, to date, the application of "click" reactions in living systems has been largely limited to extracellular targets.[5] The reasons for this are likely several. In addition to fulfilling the stability, toxicity, and chemoselectivity requirements of "click" chemistry, intracellular live-cell labeling requires reagents that can pass easily through biological membranes and kinetics that enable rapid labeling even with the low concentrations of agent that make it across the cell membrane. Additionally, a practical intracellular bioorthogonal coupling scheme would need to incorporate a mechanism by which the fluorescent tag increases in fluorescence upon covalent reaction to avoid visualizing accumulated but unreacted imaging agent (i.e. "background"). Such activatable "turn-on" probes would significantly increase the signal-to-background ratio, which is particularly relevant to imaging targets inside living cells since a stringent washout of unreacted probe is not possible.

In previous years a number of elegant probes have been introduced whose fluorescence increases after azide–alkyne cycloaddition or Staudinger ligation coupling reactions.[6] Most of these strategies utilize a reactive group intimately attached to the fluorophore thus necessitating synthesis of new fluorophore scaffolds or take advantage of a FRET (fluorescence resonant energy transfer) based activation requiring appendage of an additional molecule that can act as an energy-transfer agent. Furthermore, most probes employing these popular coupling schemes have not been used to label intracellular targets in live cells. Here we report a series of activatable "turn-on" tetrazine-linked fluorescent probes, which react rapidly through an inverse-electron-demand cycloaddition with strained dienophiles such as *trans*-cyclooctene. Upon cycloaddition, the fluorescence intensity increases substantially, in some cases by approximately 20-fold. This fluorescence "turn-on" significantly lowers background signal. We have used these novel probes for live-cell imaging of a *trans*-cyclooctene-modified taxol analogue bound to intracellular tubules. The high reaction rate coupled with fluorescence activation makes this a nearly ideal method for revealing target molecules inside living cells.

Recently, we and others have explored conjugation reactions using inverse-electron-demand Diels–Alder cycloadditions between tetrazines and highly strained dienophiles such as norbornene and *trans*-cyclooctene.[7–9] We have shown that a novel asymmetric tetrazine is quite stable in water and serum and can react with *trans*-cyclooctene at rates of approximately $10^3\,M^{-1}s^{-1}$ at 37 °C.[9] This extremely high rate constant allowed the labeling of extracellular targets at low nanomolar concentrations of tetrazine labeling agent, concentrations that are sufficiently low to enable real-time imaging of probe accummulation. Previous work from our group relied on tetrazines conjugated to highly charged carbocyanine-based near-IR-emitting fluorophores. In our efforts to explore the utility of this reaction for intracellular labeling, we conjugated 3-(4-benzylamino)-1,2,4,5-tetrazine to the succinimidyl esters of visible-light-emitting boron-dipyrromethene (BODIPY) dyes. BODIPY dyes are uncharged and lipophilic and for these reasons have seen use in intracellular applications.[10] We also wondered whether or not visible fluorophores would show electronic interactions with the tetrazine chromophores, which have absorption maxima at 500–525 nm. In fact, the tetrazine BODIPY conjugates (e.g. **1**; see Figure 1 a) exhibited strongly reduced fluorescence compared to the parent succinimidyl esters of the fluorophores. Upon reaction with a strained dienophile such as *trans*-cyclooctenol (**2**) or norbornene the fluorescence was "switched" back on.

To explore the generality of this phenomenon we reacted the benzylamino tetrazine with commercially available succinimidyl esters of 7-diethylaminocoumarin-3-carboxylic acid,

[*] Dr. N. K. Devaraj, Dr. S. Hilderbrand, R. Upadhyay, Dr. R. Mazitschek, Prof. R. Weissleder
Center for Systems Biology, Massachusetts General Hospital
Richard B. Simches Research Center
185 Cambridge Street, Suite 5.210, Boston, MA 02114 (USA)
Fax: (+1) 617-643-6133
E-mail: rweissleder@mgh.harvard.edu
Homepage: http://csb.mgh.harvard.edu

[**] We thank Dr. Justin Ragains for helpful advice and Alex Chudnovsky for assistance with tissue culture. This research was supported in part by NIH grants U01-HL080731, T32-CA79443, P50-CA86355, and RO1-EB010011.

Supporting information for this article is available on the WWW under http://dx.doi.org/10.1002/anie.200906120.

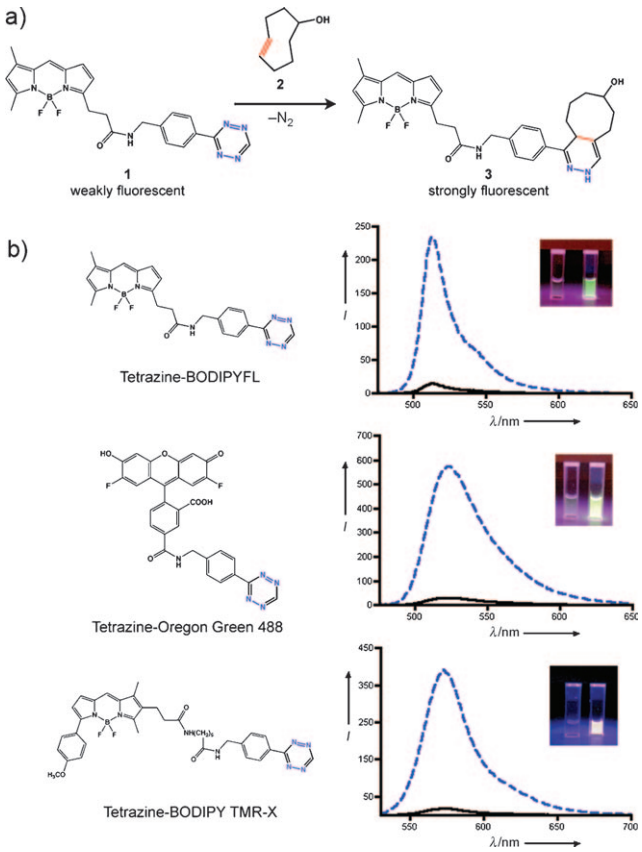

Figure 1. a) Tetrazine–BODIPY FL (**1**) reacts rapidly with *trans*-cyclooctenol (**2**) in an inverse-electron-demand Diels–Alder cycloaddition to form isomeric dihydropyrazine products **3** upon extrusion of dinitrogen and rearrangement. b) Emission spectra of various tetrazine probes (black lines) and the corresponding dihydropyrazine products (dashed blue lines). Inset images compare the visible fluorescence emission of the tetrazine probes (left cuvettes) to their corresponding dihydropyrazine products (right cuvettes) under excitation from a handheld UV lamp.

BODIPY FL, BODIPY TMR-X, Oregon Green 488 (Invitrogen), and Vivotag-680 (VT680, Visen Medical). Figure 1b shows the fluorescence emission spectra of selected dye–tetrazine conjugates before and after cycloaddition to *trans*-cyclooctenol (**2**). Table 1 lists the photophysical properties of the dyes before and after reaction. For all dyes with emission between 400–600 nm conjugation to the tetrazine caused fluorescence quenching, which was restored after reaction with dienophiles. Quenching of the fluorophore by the tetrazine is wavelength-dependent. Green- and red-emitting tetrazine dyes showed fluorescence enhancements upon cycloaddition of approximately 15- to 20-fold in PBS (phosphate-buffered saline). In contrast, the shorter-wavelength-emitting tetrazine–coumarin showed only a threefold enhancement. The green- and red-emitting tetrazine dyes also show strong fluorogenic responses in 100% fetal bovine serum (see the Supporting Information, Table S2). Near-IR-emitting dyes such as our previously used carbocyanine tetrazine–VT680 as well as tetrazine–BODIPY 650-665 (data not shown) were not quenched, explaining why this phenomenon was not observed in previous studies.

We speculate that the mechanism of fluorescence quenching may be due to resonant energy transfer between the fluorescent chromophore and the tetrazine, which has a visible absorbance maximum at 515 nm.[8] This would explain the wavelength dependence of the quenching. Another possibility could be that the quenching is the result of photoinduced electron transfer (PET) between the excited fluorophore and a potential tetrazine acceptor. Tetrazines are well known to be an electron-poor class of heterocycles, hence their utility in inverse-electron-demand cycloadditions. The PET-based mechanism would be reminiscent of the well-known quenching of fluorophores by electron-poor nitroaromatic compounds.[11] The fluorescence signals from the quenched tetrazine–BODIPY FL and tetrazine–BODIPY TMR-X conjugates vary by less than 5% between pH 9 and 3, indicating the quenching mechanism is not pH dependent. It is important to note that these fluorogenic compounds can be formed from commercially available fluorophores and that the tetrazine appears to be a sufficiently strong quencher that does not require intimate connection to the fluorophore and can achieve a quenching effect even when separated by aliphatic spacers. We are currently investigating the mechanism of quenching and designing next-generation tetrazine–fluorophores that show further enhancements of fluorescence upon cycloaddition.

Although we envision that the featured fluorogenic probes could have many applications, one use that would immediately benefit from a fluorogenic probe is the detection of target molecules inside live cells. This will allow application for determining the subcellular distribution of pharmaceutical and metabolic analogues containing a dienophile tag. To test if the fluorogenic tetrazines reported here are relevant for imaging intracellular molecular targets, we chose dienophile-modified paclitaxel (taxol, **4**) as a model system. Taxol was selected because of its tremendous clinical impact, the large body of prior work that serves as reference, and based on its well-studied ability to stabilize microtubules, providing us a well-defined intracellular structure to image.[12–15] The *trans*-cyclooctene taxol derivative

Table 1: Photophysical properties of the dyes before and after reaction with *trans*-cyclooctene (TCO).[a]

Dye	λ_{abs} [nm][b]	λ_{em} [nm][b]	Quantum yield w/o TCO[c]	Quantum yield with TCO[d]	Increase in fluorescence
tetrazine–coumarin	430	480	0.01	0.03	3.3-fold
tetrazine–BODIPY FL	505	512	0.02	0.24	15.0-fold
tetrazine–Oregon Green 488	495	523	0.04	0.82	18.5-fold
tetrazine–BODIPY TMR-X	543	573	0.02	0.40	20.6-fold
tetrazine–VT680	669	687	0.16	0.16	1.0-fold

[a] All measurements are in PBS, pH 7.4 (dye concentration 1 μM). Quantum yield measurements are in triplicate with fluorescein (in water, pH 10), Rhodamine 6G (in EtOH), or Cy5.5 in PBS as standards. [b] λ_{abs} and λ_{em} are before addition of *trans*-cyclooctene (10 μM), but there are no significant changes in these values after *trans*-cyclooctene addition. [c] Quantum yields for the tetrazine–fluorophore conjugates. [d] Quantum yields for the dihydropyrazine fluorophore products.

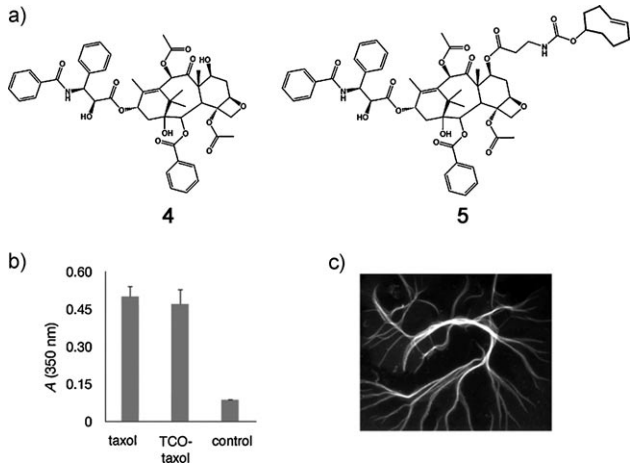

Figure 2. a) Structure of taxol (**4**) and *trans*-cyclooctene-modified taxol (**5**, TCO-taxol). b) Comparison of the ability of 10 μM taxol (**4**), *trans*-cyclooctene taxol (**5**), and a DMSO control to polymerize tubulin in the absence of GTP (polymerization assayed through absorbance at 350 nm). Note that *trans*-cyclooctene taxol (**5**) promotes polymerization similar to taxol and significantly better than a DMSO control. c) Microtubule bundles formed in the presence of *trans*-cyclooctene taxol (**5**) treated with tetrazine–BODIPY FL (**1**) and visualized by fluorescence microscopy.

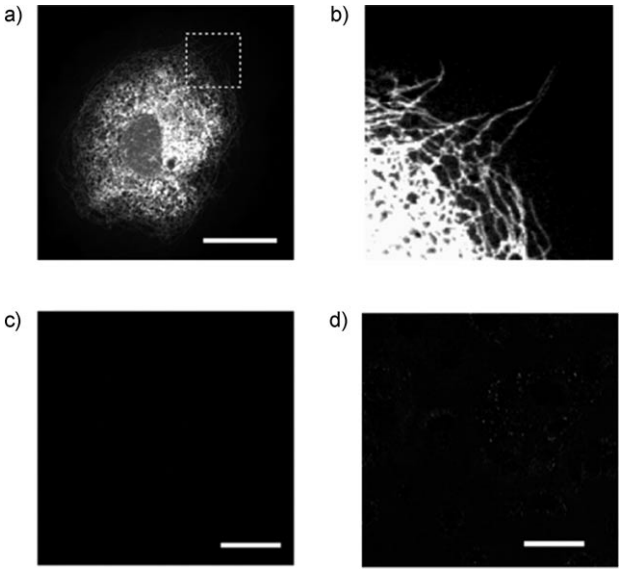

Figure 3. a) Confocal microscopy of PtK2 cells after treatment with 1 μM *trans*-cyclooctene taxol (**5**) followed by 1 μM tetrazine–BODIPY FL (**1**). Scale bar: 30 μm. b) Expansion of the section indicated by the dashed box reveals that tubular structures are clearly stained. c) Confocal microscopy of PTK2 cells after treatment with 1 μM taxol (**4**) followed by 1 μM tetrazine–BODIPY FL (**1**). Scale bar: 50 μm. d) Confocal microscopy of PTK2 cells after treatment with 1 μM *trans*-cyclooctene taxol (**5**) followed by 1 μM tetrazine–VT680. Scale bar: 50 μm.

(**5**, Figure 2) was synthesized by coupling *trans*-cyclooctene succinimidyl carbonate to 7-β-alanyl taxol by reported procedures.[13] The dienophile was introduced in the C7 position since prior structure–activity relationship studies have established that modifications at the C7 position do not significantly affect the biological activity of taxol.[13,15,16] *trans*-Cyclooctene taxol (**5**) rapidly reacts with our tetrazine probes forming isomeric dihydropyrazine products which can be detected by LC-MS (see the Supporting Information).

To test the activity of the *trans*-cyclooctene taxol analogue (**5**), we focused on the well-established ability of taxol to polymerize tubulin in the absence of GTP (guanosine triphosphate).[17] Optical density measurements at 350 nm (Figure 2b) were used to determine the degree of tubulin polymerization after exposure of tubulin monomer to taxol (**4**), *trans*-cyclooctene taxol (**5**), and a DMSO (dimethyl sulfoxide) control. Both native taxol (**4**) and *trans*-cyclooctene taxol (**5**) induce polymerization compared to a DMSO control. *trans*-Cyclooctene taxol induced tubule bundles were visualized by subsequent staining with tetrazine fluorophore probes such as tetrazine–BODIPY FL (**1**), which covalently couples to the microtubule-bound *trans*-cyclooctene taxol molecules, yielding brightly fluorescent tubule structures that can be imaged by fluorescence microscopy (Figure 2c).

For live-cell studies, PtK2 kangaroo rat kidney cells were incubated in cell media containing 1 μM *trans*-cyclooctene taxol (**5**) for 1 hour at 37 °C. PtK2 cells are commonly used in microtubule studies due to their flattened morphology.[15] After washing with media three times, the cells were exposed to media containing 1 μM tetrazine–BODIPY FL (**1**) for 20 min at room temperature. The cells were then washed and imaged on a confocal microscope (Figure 3). Intracellular structures reflecting tubule networks become readily apparent. This staining pattern corresponds to immunostaining using anti-α-tubulin (Figure S2 in the Supporting Information). Taxol is known to bind the microtubular networks of cells and there are several reports of fluorescent taxol derivatives for imaging microtubular networks.[12,13,15] Control experiments employing tetrazine–BODIPY FL (**1**) alone or with unmodified taxol (**4**) yielded minimal fluorescence background signal and demonstrate that there is little non-specific or background turn-on and that the images result from the specific tetrazine *trans*-cyclooctene cycloaddition reaction (Figure 3c). Furthermore, cells treated with *trans*-cyclooctene modified taxol (**5**) followed by highly charged non-membrane permeable tetrazine probes such as the sulfonated tetrazine–VT680 showed very little staining and an absence of tubular structures, giving further evidence that tetrazine–BODIPY FL (**1**) is able to penetrate the cell membrane and label *trans*-cyclooctene (**2**) located within the cell (Figure 3d).[8,9] Attempts to label cells with fluorescent tetrazine–taxol conjugates led to nonspecific weak staining signals (Figure S3 in the Supporting Information).

In conclusion we have developed a robust method for the bioorthogonal tagging and imaging of targets inside living cells. Fluorogenic tetrazine probes react specifically and rapidly with strained dienophiles such as *trans*-cyclooctene (**2**). The ability of these probes to show fluorescence "turn-on" upon cycloaddition is a major advantage especially for applications where probe washout is not desired or possible. We imagine that this method will be useful for applications requiring the imaging of the intracellular distribution of tagged small molecules. We are currently exploring imaging

other dienophile-containing small molecules for therapeutic targets both in vitro with live cells and in vivo using relevant animal models.

Received: October 30, 2009
Revised: January 20, 2010
Published online: ■■ ■■, 2010

Keywords: bioorthogonal reactions · cycloaddition · fluorogenic tags · imaging · tetrazine

[1] H. C. Kolb, M. G. Finn, K. B. Sharpless, *Angew. Chem.* **2001**, *113*, 2056 – 2075; *Angew. Chem. Int. Ed.* **2001**, *40*, 2004 – 2021; V. V. Rostovtsev, L. G. Green, V. V. Fokin, K. B. Sharpless, *Angew. Chem.* **2002**, *114*, 2708 – 2711; *Angew. Chem. Int. Ed.* **2002**, *41*, 2596 – 2599.

[2] A. E. Speers, G. C. Adam, B. F. Cravatt, *J. Am. Chem. Soc.* **2003**, *125*, 4686 – 4687; A. Salic, T. J. Mitchison, *Proc. Natl. Acad. Sci. USA* **2008**, *105*, 2415 – 2420; W. G. Lewis, L. G. Green, F. Grynszpan, Z. Radic, P. R. Carlier, P. Taylor, M. G. Finn, K. B. Sharpless, *Angew. Chem.* **2002**, *114*, 1095 – 1099; *Angew. Chem. Int. Ed.* **2002**, *41*, 1053 – 1057; K. E. Beatty, F. Xie, Q. Wang, D. A. Tirrell, *J. Am. Chem. Soc.* **2005**, *127*, 14150 – 14151; J. Gubbens, E. Ruijter, L. E. de Fays, J. M. Damen, B. de Kruijff, M. Slijper, D. T. Rijkers, R. M. Liskamp, A. I. de Kroon, *Chem. Biol.* **2009**, *16*, 3 – 14; T. L. Hsu, S. R. Hanson, K. Kishikawa, S. K. Wang, M. Sawa, C. H. Wong, *Proc. Natl. Acad. Sci. USA* **2007**, *104*, 2614 – 2619.

[3] S. T. Laughlin, J. M. Baskin, S. L. Amacher, C. R. Bertozzi, *Science* **2008**, *320*, 664 – 667; A. B. Neef, C. Schultz, *Angew. Chem.* **2009**, *121*, 1526 – 1529; *Angew. Chem. Int. Ed.* **2009**, *48*, 1498 – 1500; X. H. Ning, J. Guo, M. A. Wolfert, G. J. Boons, *Angew. Chem.* **2008**, *120*, 2285 – 2287; *Angew. Chem. Int. Ed.* **2008**, *47*, 2253 – 2255; J. M. Baskin, J. A. Prescher, S. T. Laughlin, N. J. Agard, P. V. Chang, I. A. Miller, A. Lo, J. A. Codelli, C. R. Bertozzi, *Proc. Natl. Acad. Sci. USA* **2007**, *104*, 16793 – 16797.

[4] J. A. Prescher, C. R. Bertozzi, *Nat. Chem. Biol.* **2005**, *1*, 13 – 21.

[5] J. M. Baskin, C. R. Bertozzi, *QSAR Comb. Sci.* **2007**, *26*, 1211 – 1219.

[6] K. Sivakumar, F. Xie, B. M. Cash, S. Long, H. N. Barnhill, Q. Wang, *Org. Lett.* **2004**, *6*, 4603 – 4606; Z. Zhou, C. J. Fahrni, *J. Am. Chem. Soc.* **2004**, *126*, 8862 – 8863; M. J. Hangauer, C. R. Bertozzi, *Angew. Chem.* **2008**, *120*, 2428 – 2431; *Angew. Chem. Int. Ed.* **2008**, *47*, 2394 – 2397; G. A. Lemieux, C. L. De Graffenried, C. R. Bertozzi, *J. Am. Chem. Soc.* **2003**, *125*, 4708 – 4709.

[7] M. L. Blackman, M. Royzen, J. M. Fox, *J. Am. Chem. Soc.* **2008**, *130*, 13518 – 13519; R. Pipkorn, W. Waldeck, B. Didinger, M. Koch, G. Mueller, M. Wiessler, K. Braun, *J. Pept. Sci.* **2009**, *15*, 235 – 241.

[8] N. K. Devaraj, R. Weissleder, S. A. Hilderbrand, *Bioconjugate Chem.* **2008**, *19*, 2297 – 2299.

[9] N. K. Devaraj, R. Upadhyay, J. B. Haun, S. A. Hilderbrand, R. Weissleder, *Angew. Chem.* **2009**, *121*, 7147 – 7150; *Angew. Chem. Int. Ed.* **2009**, *48*, 7013 – 7016.

[10] L. Cole, D. Davies, G. J. Hyde, A. E. Ashford, *J. Microsc.* **2000**, *197*, 239 – 249; J. Farinas, A. S. Verkman, *J. Biol. Chem.* **1999**, *274*, 7603 – 7606; E. W. Miller, L. Zeng, D. W. Domaille, C. J. Chang, *Nat. Protoc.* **2006**, *1*, 824 – 827; N. Takahashi, T. Nemoto, R. Kimura, A. Tachikawa, A. Miwa, H. Okado, Y. Miyashita, M. Iino, T. Kadowaki, H. Kasai, *Diabetes* **2002**, *51 Suppl 1*, 25S – 8; K. Viht, K. Padari, G. Raidaru, J. Subbi, I. Tammiste, M. Pooga, A. Uri, *Bioorg. Med. Chem. Lett.* **2003**, *13*, 3035 – 3039.

[11] J. V. Goodpaster, V. L. McGuffin, *Anal. Chem.* **2001**, *73*, 2004 – 2011; Y. Kim, Z. Zhu, T. M. Swager, *J. Am. Chem. Soc.* **2004**, *126*, 452 – 453.

[12] J. A. Evangelio, M. Abal, I. Barasoain, A. A. Souto, M. P. Lillo, A. U. Acuna, F. Amat-Guerri, J. M. Andreu, *Cell Motil. Cytoskeleton* **1998**, *39*, 73 – 90.

[13] R. Guy, Z. Scott, R. Sloboda, K. Nicolaou, *Chem. Biol.* **1996**, *3*, 1021 – 1031.

[14] J. J. Manfredi, J. Parness, S. B. Horwitz, *J. Cell Biol.* **1982**, *94*, 688 – 696; K. C. Nicolaou, W. M. Dai, R. K. Guy, *Angew. Chem.* **1994**, *106*, 38 – 69; *Angew. Chem. Int. Ed. Engl.* **1994**, *33*, 15 – 44; E. K. Rowinsky, L. A. Cazenave, R. C. Donehower, *J. Natl. Cancer Inst.* **1990**, *82*, 1247 – 1259.

[15] A. A. Souto, A. U. Acuna, J. M. Andreu, I. Barasoain, M. Abal, F. AmatGuerri, *Angew. Chem.* **1995**, *107*, 2910 – 2912; *Angew. Chem. Int. Ed. Engl.* **1995**, *34*, 2710 – 2712.

[16] S. H. Chen, J. Kant, S. W. Mamber, G. P. Roth, J. M. Wei, D. Marshall, D. M. Vyas, V. Farina, A. Casazza, B. H. Long, W. C. Rose, K. Johnston, C. Fairchild, *Bioorg. Med. Chem. Lett.* **1994**, *4*, 2223 – 2228; W. Mellado, N. F. Magri, D. G. Kingston, R. Garcia-Arenas, G. A. Orr, S. B. Horwitz, *Biochem. Biophys. Res. Commun.* **1984**, *124*, 329 – 336.

[17] M. L. Shelanski, F. Gaskin, C. R. Cantor, *Proc. Natl. Acad. Sci. USA* **1973**, *70*, 765 – 768; P. B. Schiff, S. B. Horwitz, *Biochemistry* **1981**, *20*, 3247 – 3252.

Communications

Labeling of Live Cells

N. K. Devaraj, S. Hilderbrand,
R. Upadhyay, R. Mazitschek,
R. Weissleder* _____ ■■■■–■■■■

Bioorthogonal Turn-On Probes for Imaging Small Molecules inside Living Cells

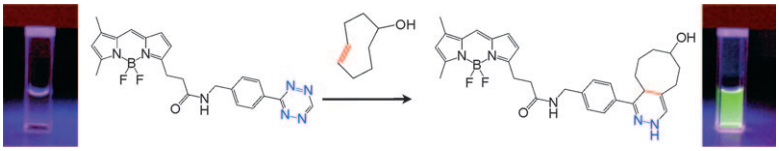

Glowing tags: A series of activatable ("turn-on") tetrazine-conjugated fluorescent probes was developed, which react rapidly in an inverse-electron-demand [4+2] cycloaddition with strained dienophiles such as *trans*-cyclooctene, thereby strongly increasing the fluorescence intensity (see picture). The novel turn-on probes were applied for intracellular live-cell imaging of a microtubuli-binding *trans*-cyclooctene modified taxol.

Angewandte Chemie
Eine Zeitschrift der Gesellschaft Deutscher Chemiker

Supporting Information

69451 Weinheim, Germany

Bioorthogonal Turn-On Probes for Imaging Small Molecules inside Living Cells**

*Neal K. Devaraj, Scott Hilderbrand, Rabi Upadhyay, Ralph Mazitschek, and Ralph Weissleder**

anie_200906120_sm_miscellaneous_information.pdf

Supporting Information

Materials and Methods

General considerations. All chemicals were purchased from Sigma Aldrich, unless noted, and were used as received. The amine reactive cyanine dye VivoTag 680 (VT680) was purchased from Visen Medical (Bedford, MA). Amine reactive succinimidyl esters of BODIPY FL, BODIPY TMR-X, Oregon Green 488, 7-N, N-diethylaminocoumarin, anti-α-tubulin mouse IgG_1, and Alexa Fluor 647 $F(ab')_2$ fragment of goat anti-mouse IgG were purchased from Invitrogen (Carlsbad, CA). All solvents were of reagent grade or higher and were used without further purification. Analytical HPLC and LC/MS were performed on a Waters 2695 HPLC equipped with a 2996 diode array detector, a Micromass ZQ4000 ESI-MS module, and a Grace-Vydac RPC18 column (model 218TP5210) at a flow rate of 0.3 mL/min. For all HPLC runs, solvent A consists of water with 0.1% TFA and solvent B is composed of acetonitrile with 10% water and 0.1% TFA. Preparative high performance liquid chromatography (HPLC) was performed on a Varian 210 instrument equipped with a 335 diode array detector and a Varian Pursuit XRs 10 C18 250 X 21.2 mm column using a flow rate of 21 mL/min. Buffer A consists of water with 0.1% TFA. Buffer B is acetonitrile containing 10% water and 0.1% TFA. Absorption spectra were collected on a Varian Cary 50-Bio UV/visible spectrophotometer and fluorescence data were collected on a Varian Cary Eclipse fluorescence spectrophotometer. Quantum yield measurements were performed in triplicate with an observed error of 8% or less for each set of measurements using established procedures.[4] Excitation wavelengths of 425, 470, 470, 520, and 640 nm were used for the quantum yield measurements on the coumarin, Oregon Green 488, BODIPY FL, BODIPY TMR-X, and VT680-tetrazine conjugates, respectively. Fluorescein[1] (in pH 10 water) was used as the standard for the coumarin, Oregon Green 488, and BODIPY FL conjugates. Whereas rhodamine 6G[2] (in EtOH) and Cy 5.5[3] (in PBS) were the fluorescence standards for the BODIPY TMR-X, and VT680-tetrazine conjugates, respectively. All fluorescence activation studies were performed in triplicate. The pH dependence on the quenching of the tetrazine-fluorophore conjugates was measured in triplicate using a 10 mM phosphate/citric acid buffer system over a pH range from 9.0 to 3.0. Low resolution electrospray mass spectrometry data were collected on a Micromass ZQ4000 instrument.

Synthetic Methods

Tetrazine amine (1) and (*E*)-cyclooct-4-enyl 2,5-dioxopyrrolidin-1-yl carbonate were synthesized as previously reported by our group.[5] 7-β-alanyltaxol was synthesized as previously reported by Nicolaou.[6]

Trans-cyclooctene Taxol synthesis

The *trans*-cyclooctene taxol derivative was synthesized using a modification of a previously reported procedure.[6] 7-β-alanyltaxol was dissolved in anhydrous acetonitrile and reacted overnight at room temperature with (*E*)-cyclooct-4-enyl 2,5-dioxopyrrolidin-1-yl carbonate. After reaction, the acetonitrile was removed by rotary evaporation and the product isolated by column chromatography (17 mg). ^{1}HNMR (400

MHz $CDCl_3$): δ 8.14-8.06 (d, 2H), 7.8-7.7 (d, 2H), 7.66-7.56 (t, 1H), 7.54-7.3 (m, 10H) 7.1-7.0 (d, 1H), 6.3-6.1 (m, 2H), 5.85-5.75 (d, 1H), 5.7-5.6 (d, 1H), 5.6-5.4 (m, 3H), 5-4.85 (d, 1H), 4.85-4.75 (m, 1H), 4.4-4.25 (m, 2H), 4.25-4.1 (d 1H), 3.95-3.85 (d, 1H), 3.65-3.55 (d, 1H), 1-3 (m 38H). [M+H]+ calc mass 1077.5 found mass 1077.7, [M+Na]+ calc mass 1099.4 found mass 1099.6

General procedure for the synthesis of the tetrazine fluorophore conjugates.
To a solution of 3-(4-benzylamino)-1,2,4,5-tetrazine (10 µmol) in anhydrous DMF (0.5 mL) was added the succinimidyl ester of the appropriate fluorophore (2.5 µmol) and triethylamine (10 µmol). The resulting solution was allowed to shake overnight in the dark. The crude reaction mixture was then purified by preparative reverse phase HPLC using a gradient from 0 to 100% buffer B. The identity and purity of the conjugates were confirmed by electrospray mass spectrometry and analytical HPLC, respectively.

Table S1. Mass spectrometry data for tetrazine fluorophore conjugates before and after reaction with *trans*-cyclooctenol and *trans*-cyclooctenol taxol

compound	ionic species	formula	calcd. mass	found mass
Tetrazine-BODIPY FL	[M+H]+ [M+Na]+	$C_{23}H_{23}BF_2N_7O$+ $C_{23}H_{22}BF_2N_7NaO$+	462.20 484.18	462.2 484.2
Tetrazine-BODIPY TMR-X	[M+H]+ [M+Na]+	$C_{36}H_{40}BF_2N_8O_3$+ $C_{36}H_{39}BF_2N_8NaO_3$+	681.33 703.31	681.4 703.5
Tetrazine-Oregon Green 488	[M+H]+	$C_{30}H_{18}F_2N_5O_6$+	582.12	582.3
Tetrazine-BODIPY FL + *trans*-cyclooctenol	[M+H]+	$C_{31}H_{37}BF_2N_5O_2$+	560.30	560.4
Tetrazine-BODIPY TMR-X + *trans*-cyclooctenol	[M+H]+	$C_{44}H_{54}BF_2N_6O_4$+	779.43	779.5
Tetrazine-Oregon Green 488 + *trans*-cyclooctenol	[M+H]+	$C_{38}H_{32}F_2N_3O_7$+	680.22	680.3
Tetrazine-BODIPY FL + *trans*-cyclooctene taxol	[M+H]+	$C_{82}H_{91}BF_2N_7O_{18}$+	1510.65	1510.7

Cell Culture
Kangaroo rat kidney epithelial cell line PtK2 was selected for all experiments and was obtained from ATCC. The cell line was maintained in a standard ATCC formulated Eagle's minimum essential medium supplemented with 10% fetal bovine serum.

Confocal Microscopy
Cells were grown on break away glass chamber slides and washed 3 times after administering any reagent. The wash step was necessitated due to the set-up of our chambered slides. The chamber which separates the the different sections allowing for

experiments to be done in parallel and containment of labeling solution must be broken off prior to imaging (we use a water immersion microscope objective). To avoid cross contamination, the chambers are drained and washed prior to separating the chamber from the slide. A multichannel upright laser-scanning confocal microscope (FV1000; Olympus) was used to image live cells with a 60X water immersion objective lens. Image collection and fluorophore excitation with lasers at 488 nm (BODIPY FL) and at 750 nm (producing a 2-photon excitation of the Hoechst nuclear stain), were done serially to avoid cross talk between channels. Data were acquired with Fluoview software (version 4.3; Olympus) and image stacks were processed and analyzed with ImageJ software (version 1.41, Bethesda MD).

Tubulin polymerization assay

Tubulin polymerization was monitored using an adaptation of the original method of Shelanski et al.[7] Lyophilized bovine brain tubulin (Cytoskeleton Inc.) was suspended at 2.5 mg/mL in PEM buffer (80 mM Na-PIPES pH 6.9, 1 mM $MgCl_2$ and 1 mM EGTA). To 19 µL of tubulin solution was added 1 µL of a 200 µM DMSO solution of either taxol, trans-cyclooctene taxol, or control (DMSO only). The solutions were warmed to 37°C for 20 minutes, allowed to cool at 4°C for 5 minutes, and then the absorption at 350 nm was measured.

Cell labeling experiments

In a typical experiment, PTK2 cells were first incubated with *trans*-cyclooctene taxol (1 µM) in serum for 1 hour at 37°C. Cells were then washed with PBS, and incubated with tetrazine-BodipyFL (1 µM also in serum for 37°C) for 20 minutes.

Immunostaining

PTK2 cells were fixed for 5 minutes with cold methanol (-20°C). Cells were then exposed to a solution of perm/wash buffer (BD Biosciences Phosflow Perm/Wash Buffer I) containing 1 µg/mL anti-α-tubulin mouse IgG_1 for 30 minutes. After washing the cells with perm/wash buffer (2 times) the cells were exposed to a solution of perm/wash buffer containing 10 µg/mL of Alexa Fluor 647 $F(ab')_2$ fragment of goat anti-mouse IgG followed by a final washing withe perm/wash buffer (2 times)

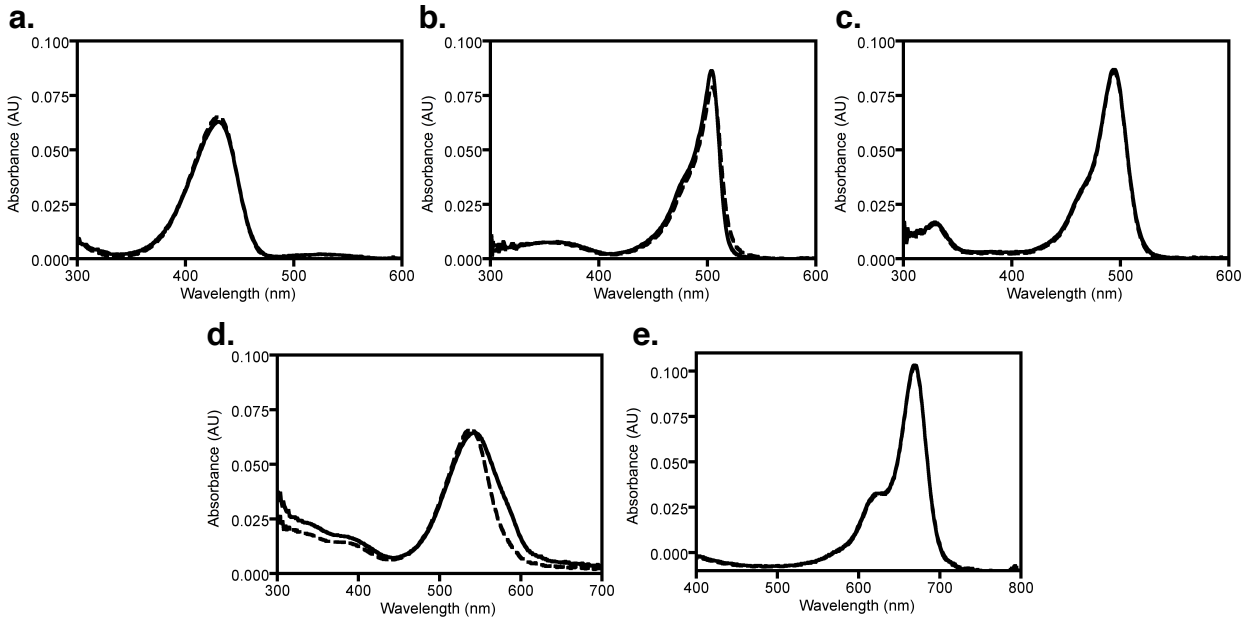

Figure S1. Absorbance spectra for 1 μM solutions of the tetrazine-fluorophore constructs before (solid lines) and after (dashed lines) reaction with 10 equivalents of *trans*-cyclooctenol in PBS. Panels **a-e** correspond to the tetrazine-coumarin, tetrazine-BODIPY FL, tetrazine-Oregon Green 488, tetrazine BODIPY TMR-X, and tetrazine-VT680, respectively.

Table S2. Fluorescence response of 1 μM solutions of the tetrazine-fluorophore constructs after reaction with 10 equiv. of *trans*-cyclooctenol in 100% fetal bovine serum

compound	fluorescence activation (increase in integrated emission)
Tetrazine-BODIPY FL	14-fold
Tetrazine-Oregon Green 488	12-fold
Tetrazine-BODIPY TMR-X	11-fold

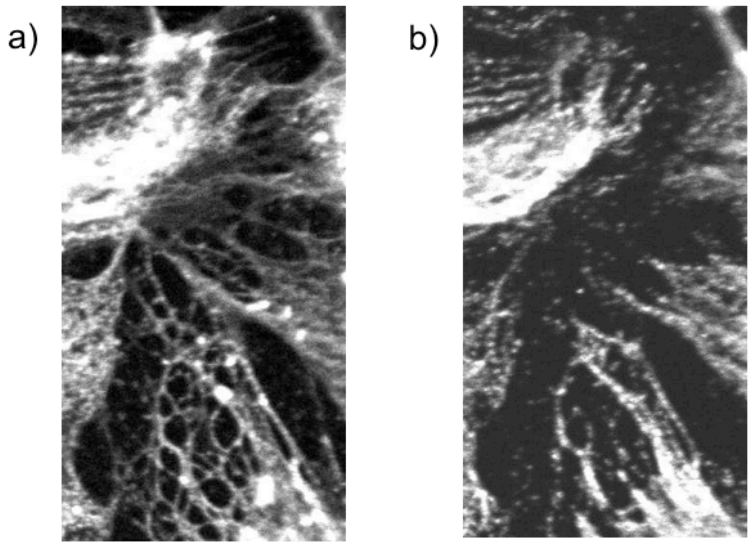

Figure S2: fluorescence microscopy of PTK2 cells stained by *trans*-cyclooctene taxol/ BODIPYFL-tetrazine (a) followed by fixation and immunostaining with anti-α-tubulin (b). The emission wavelengths were 510 nm and 665 nm respectively.

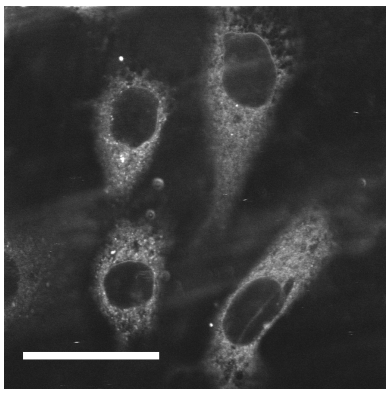

Figure S3: PTK2 cells after 20 minute exposure to a 1 μM solution of taxol conjugated to tetrazine-BODIPY FL. Scale: 30 μm.

References

[1] Velapoldi, R. A., Tonnesen, H. H. *J Fluoresc* **2004**, *14*, 465-472.
[2] Fischer, M., Georges, J. *Chem. Phys. Lett.* **1996**, *260*, 115-118.
[3] Mujumdar, S. R., Mujumdar, R. B., Grant, C. M., Waggoner, A. S. *Bioconjug Chem* **1996**, *7*, 356-362.
[4] Demas, J. N., GA, C. *J. Phys. Chem.* **1971**, *75*, 991-&.
[5] Devaraj, N. K., Weissleder, R., Hilderbrand, S. A. *Bioconjug Chem* **2008**, *19*, 2297-2299; Devaraj, N. K., Upadhyay, R., Haun, J. B., Hilderbrand, S. A., Weissleder, R. *Angew Chem Int Ed Engl* **2009**, *48*, 7013-7016.

[6] Guy, R., Scott, Z., Sloboda, R., Nicolaou, K. *Chem Biol* **1996**, *3*, 1021-1031.
[7] Shelanski, M. L., Gaskin, F., Cantor, C. R. *Proc Natl Acad Sci U S A* **1973**, *70*, 765-768.